Physicochemical properties of monometallic Rh and Ni and bimetallic RhNi catalyst materials supported on unmodified and yttrium-modified alumina

R. Palcheva, I. Shtereva, Y. Karakirova, G. Tyuliev, S. Damyanova*

Institute of Catalysis, Bulgarian Academy of Sciences, G. Bonchev St., Bldg. 11, 1113 Sofia, Bulgaria

The effect of Y_2O_3 addition to γ-alumina carrier on the structure and surface and reductive properties of supported monometallic Rh and Ni bimetallic RhNi materials was studied. Various techniques for physicochemical characterization were used, such as N_2 adsorption-desorption isotherms, XRD, UV-vis DRS, XPS, EPR, and TPR. XRD, UV-vis DRS, and XPS results of calcined samples showed the presence of Ni^{2+} ions in different environment: octahedral and tetrahedral coordination. Well-dispersed yttrium and rhodium oxide species were detected. EPR and TPR data indicated a strong interaction between Ni and yttria, as revealed by higher temperature of reduction of nickel oxide species. Rh promoting effect on the reduction of Ni oxide species was related to hydrogen spillover effect of the noble metal.

Key words: nickel catalysts, rhodium, yttrium, characterization.

INTRODUCTION

Due to high availability and low cost, alumina-supported nickel catalyst materials have been widely used for hydrogen production by reforming processes of ethanol [1,2] and for synthesis gas or hydrogen-rich synthesis gas production by reforming of methane with CO_2 [3]. On the other hand, methane and carbon dioxide are greenhouse gases that cause the global climate change and considerable attention has been given to control and utilize these gases [4,5]. It is well known that Ni-based catalysts supported on alumina suffer from carbon deposition over the active phase. Different studies have been focused on problems how to eliminate coke formation on Ni catalysts including use of suitable additives or supports to modify the physicochemical properties of Ni/Al_2O_3 with beneficial features, such as high metal dispersion, high number of basic sites, and superior reducible nature [6–8]. Another promising alternative to obtain highly active and coke resistant Ni-based catalysts is addition of small amount of noble metal [9–12]. The aim of the present work was to study the effect of yttrium addition to γ-alumina carrier and of Rh introduction to supported Ni catalysts on their structure and surface and reductive properties. Sample physicochemical properties were examined by applying N_2 adsorption-desorption isotherms, X-ray diffraction (XRD), UV-vis diffuse reflectance spectroscopy (UV-vis DRS), X-ray photoelectron spectroscopy (XPS), electron paramagnetic resonance (EPR), and temperature-programmed reduction (TPR).

EXPERIMENTAL

Sample preparation

Modified alumina support with yttrium was prepared by impregnation of γ-Al_2O_3 with an aqueous solution of $Y(NO_3)_3.6H_2O$. Monometallic Ni and Rh catalysts were prepared by impregnation of unmodified and yttrium modified alumina with aqueous solution of $Ni(NO_3)_2.6H_2O$ and ethanol solution of $RhCl_3.3H_2O$ salt, respectively. Supported bimetallic NiRh samples were prepared by co-impregnation of unmodified and modified alumina with solutions of rhodium chloride and nickel nitrate salts in ethanol. Obtained solids were dried at 110 °C for 12 h and calcined at 550 °C for 4 h. The theoretical content of Y, Ni, and Rh was 10, 10, and 1 wt.%, respectively. The samples were denoted as Y-Al, Ni/Al, Rh/Al, Ni/Y-Al, RhNi/Al, and RhNi/Y-Al.

Methods

N_2 adsorption-desorption isotherms of samples were recorded at 77 K by means of a Quantachrome Instruments NOVA 1200e (USA) 3000 apparatus. Beforehand the samples were outgassed under vacuum at 200 °C for 18 h. The surface area was calculated according to the BET method. XRD analysis was performed according to step scanning procedure (step size 0.02°; 0.5 s) with a computerized Seifert 3000 diffractometer, using Ni-filtered CuKα (λ = 0.15406 nm) radiation and a PW 2200 Bragg-Brentano θ/2θ goniometer equipped with a

bent graphite monochromator and an automatic slit. The assignment of the various crystalline phases was based on JPDS powder diffraction file cards. UV-vis DRS spectra of the samples were recorded in the range of 200–800 nm at room temperature using a Varian Cary 5000 UV-vis spectrometer equipped with an integration sphere. XPS measurements of the samples were carried out on an ESCALAB-MkII (VG Scientific) spectrometer with a base pressure in the analysis chamber of $\sim 10^{-8}$ Pa. The spectra were excited with an Al Kα radiation (hν = 1253.6 eV) at total instrumental resolution of ~ 0.9 eV as measured by FWHM of Ag $3d_{5/2}$ photoelectron line. The binding energy (BE) scale of the spectrometer was calibrated with respect to the Au $4f_{7/2}$ peak of gold fixed at 83.98 eV and the BE's of O 1s, Al 2p, Ni 2p, Y 3d, and Rh 3d electrons were referenced to the O1s band at 531.5 eV. Peak decomposition was performed using Casa XPS program (Casa Software, UK) assuming 85/15 Gaussian/Lorentzian product function. EPR spectra of calcined (550 °C in air) and reduced (550 °C in 10% H_2/N_2 flow) samples were recorded as a first deri-vative of the absorption signal of JEOL JES-FA 100 EPR spectrometer at room temperature. The spectrometer operated in X-band equipped with a standard TE_{011} cylindrical resonator. The samples were placed in a special quartz reactor and fixed in the cavity centre. A variable temperature controller ES-DVT4 was used to permit detection of EPR spectra at temperatures from 123 to 298 K. Desired temperature could be easily obtained by moving liquid nitrogen at a certain temperature controlled by the EPR spectrometer data system computer to the sample area. The reduction temperature of the various phases in the oxide form of the samples was determined by the method of TPR. The reducing mixture containing 10% H_2 in Ar was deoxygenated over Pt/asbestos filter at 130 °C, dried in a molecular sieve 5A filter, and then fed into the a tubular quartz reactor at a flow rate of 25 cm^3/min. The program started from room temperature at a ramp rate of 10 deg/min up to 1000 °C. Catalyst sample amount charged in the reactor was 0.1 g. The TPR set-up was equipped with a thermal conductivity detector.

RESULTS AND DISCUSSION

Structure and surface properties

Nitrogen adsorption-desorption isotherms of calcined samples (not shown) were classified as a type IV isotherm according to IUPAC, which is typical of mesoporous materials [13]. Specific surface area (S_{BET}), total pore volume (V_p), and average pore diameter (D_p) values are summarized in Table 1.

Table 1. Textural properties of calcined monometallic and bimetallic RhNi samples

Sample	S_{BET} (m^2/g)	Vp (cm^3/g)	Pore diameter (nm)
Al_2O_3	232	0.90	15.5
Y-Al	183	0.79	17.2
Ni/Al	187	0.55	11.7
Ni/Y-Al	163	0.66	16.2
Rh/Y-Al	185	0.72	15.7
NiRh/Al	161	0.65	16.2
NiRh/Y-Al	171	0.70	16.2

A decrease in specific surface area and pore volume of the alumina carrier was observed after addition of yttrium or nickel (from 232 to 183 and 187 m^2/g for Y-Al and Ni/Al, respectively, Table 1) due to blockage of alumina pores by yttrium or nickel oxide species. The S_{BET} of modified Y-Al support continued to decrease for $Y-Al_2O_3$-supported monometallic Ni and Rh samples and it is more obvious with the former one. The bimetallic NiRh samples have the lowest specific surface area. It is interesting to note that with exception of Ni/Al the mean pore diameter of the supported samples is higher than that of pure alumina (Table 1). Probably, this is caused by the presence of particles with larger pores and owing to possible blockage of the small pores by yttrium oxide species.

XRD patterns of unmodified and Y-modified alumina and supported monometallic and bimetallic samples are shown in figure 1. Pure alumina exhibited peaks at 2θ = 37.2^o, 39.7^o, 46.2^o, and 66.4^o, which are due to γ-Al_2O_3 (JCPDS 86-1410). Modification of alumina with yttrium or addition of nickel and/or Rh led to a change of intensity and modification of the shape of the alumina lines because of changes in crystallinity of the samples.
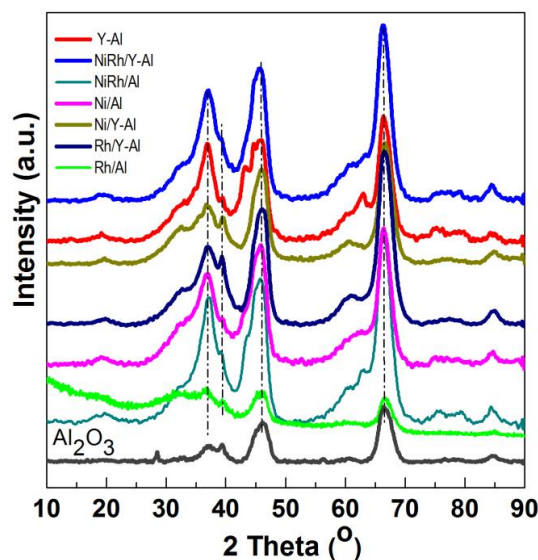
Fig. 1. XRD of supported monometallic Rh and Ni and bimetallic RhNi samples.

Diffraction lines of Y_2O_3 at $2\theta = 33.77^o$, 48.54^o, and 57.6^o (JCPDS 65-3178) were not detected in yttrium modified samples, which is an indication of the amorphous nature of the compound. In spite of the absence of peaks characteristic of $NiAl_2O_4$ phase, the presence of some surface spinel species cannot be excluded. In addition, the peaks of $NiAl_2O_4$ overlap with those of γ-Al_2O_3. For Ni/Al and NiRh/Y-Al samples XRD lines at $2\theta = 37^o$, 43.2^o, 62.9^o, and 76° are registered, which could be related to the presence of cubic NiO species (JCPDS 47-1049). However, these lines were not definitely detected with other samples. Since the main characteristic peaks of rhodium oxide species in the 2θ interval of 16–18° [14] were absent, it could be assumed that these species were well dispersed.

UV-vis DR spectra of calcined samples in the wavelength ranges of 200−800 nm and 500−800 nm are displayed in figure 2. Supported bimetallic RhNi/Y-Al sample manifested a strong absorption at 200−350 nm with a maximum at about 260 nm related to $O^{2-} \rightarrow Ni^{2+}$ charge transfer transition.
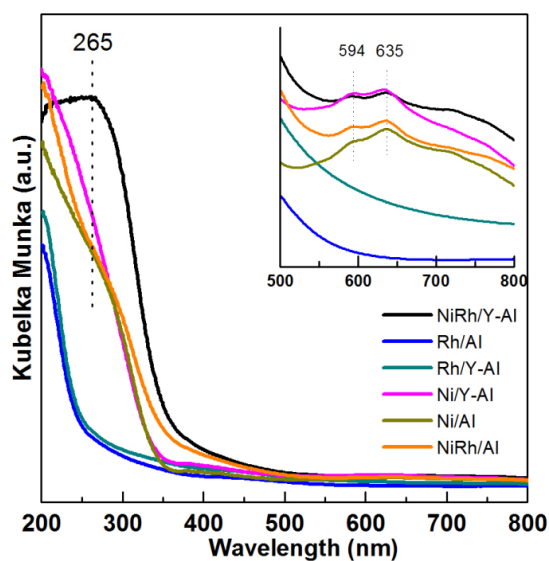
Fig. 2. UV-vis-DRS of supported monometallic Rh and Ni and bimetallic RhNi samples.

A doublet at 594 and 635 nm in the wavelength range of 500−800 nm (Fig. 2) indicates presence of Ni^{2+} ions in tetrahedral coordination of $NiAl_2O_4$ spinel like structure [15]. A broad absorption at about 720−780 nm means that Ni^{2+} ions are in octahedral coordination that is typical of NiO species. It can be concluded that the nickel ions occurred in different environment: tetrahedral and octahedral coordination.

Binding energy (BE) values of Y $3d_{5/2}$, Ni $2p_{3/2}$, and Rh $3d_{5/2}$ as well as XPS atomic ratios for calcined samples are listed in Table 2. The BE values of Y $3d_{5/2}$ electrons for Y-containing samples (158.8−159.2 eV) are higher compared to that of the bulk Y_2O_3 (157.9 eV, Table 2) which should be related to certain interaction of supported yttrium oxide species with alumina or with Rh or Ni. For Ni/Al sample the BE of Ni $2p_{3/2}$ electrons at 856.4 eV characterizes the Ni^{2+} ions in nickel oxide species, which can be ascribed to the presence of dispersed NiO species as well as of surface $NiAl_2O_4$ like species [16,17]. This is in accordance with the UV-vis DRS results (Fig. 2). However, there is some increase of the BE value of Ni $2p_{3/2}$ to 857.0 eV for NiRh/Y-Al sample, most likely due to a change in coordination and/or reflection effects in the presence of Rh and Y oxide species.

The BE values of Rh $3d_{5/2}$ electrons at 310.0–310.4 eV could be ascribed to Rh^{3+} species [18], though these values are slightly higher than that of bulk Rh_2O_3 (309.0 eV). The observed shift in binding energy values may arise from a smaller size of the supported rhodium oxide species.

XPS atomic ratios calculated from the intensities of the peak normalized by atomic sensitivity factor [19] are summarized in Table 2. Nickel oxide dispersion on alumina increased after introduction of the noble metal to Ni/Al. However, the presence of Y in monometallic Ni/Y-Al and in bimetallic RhNi/Y-Al caused a decrease in the XPS atomic Ni/Al + Y + Rh ratio values due to some agglomera-

Table 2. XPS characteristics of calcined monometallic Rh and Ni and bimetallic RhNi samples supported on unmodified and yttrium modified alumina

Sample	Y $3d_{5/2}$	Ni $2p_{3/2}$	Rh $3d_{5/2}$	Y/Al+Ni+Rh	Ni/Al+Y+Rh	Rh/Al+Y+Ni
b. Y_2O_3	157.9	-		-	-	-
Y-Al	159.2	-		0.074	-	-
Ni/Al	-	856.4		-	0.053	-
Ni/Y-Al	158.8	856.4		0.067	0.051	-
Rh/Al	-	-	310.0	-	-	0.005
Rh/Y-Al	159.1	-	310.2	0.070	-	0.005
NiRh/Al	-	856.7	310.4	-	0.058	0.003
NiRh/Y-Al	158.8	857.0	310.1	0.058	0.048	0.003

tion of nickel oxide species. Yttrium oxide species were well dispersed on pure alumina. However, addition of other elements led to a decrease of the accessibility of Y-containing species, which is more pronounced for the bimetallic RhNi/Y-Al sample (Table 2). Rh oxide species were well dispersed on the surface of unmodified and Y-modified alumina. A decrease of the atomic XPS Rh/Al+Y+Ni values with the bimetallic RhNi samples was observed (Table 2), probably due to some Rh coverage, bearing in mind nickel higher concentration. It has been reported [20] that yttrium oxide species had no important impact on oxidation state and dispersion of metallic centres, but substantially altered support acid-base properties.

Reductive properties

EPR spectra of reduced Ni/Al_2O_3, $Ni-Y/Al_2O_3$, $Ni-Rh/Al_2O_3$, and $Ni-Rh/Y-Al_2O_3$ samples at room temperature are given in figure 3. The spectra consist of two overlapping EPR signals denoted as Si1 and Si2. A narrow signal Si1 detected in the spectrum of Ni/Al_2O_3 is characterized by a g factor of 2.1993 and a linewidth of 32.6 mT. In the presence of yttrium and rhodium the *g* factor decreased to 2.1676 and 2.1480, respectively, and the value of the linewidth increased to about $42-46$ mT for Si1 because of change in atom surrounding. Based on previous EPR studies of supported Ni samples the signal Si1 can be assigned to Ni^{2+} ions in octahedral symmetry [21−23]. The electronic configuration of Ni^{2+} is d^8 and postulated coupling would lead to a spin-paired system. This signal probably had never been detected in samples containing only nickel ions. Thus, it can be stated that signal Si1 is due to the presence of paramagnetic species evidently related to the interaction among aluminium, yttrium or rhodium, and Ni^{2+} ions. A broader Si2 line in Ni-Al sample has g value of 2.3791 and linewidth of 102.8 mT. The EPR parameters of this signal were changed after modification of the sample with yttrium and rhodium to g of 2.2299 and 2.2195 and to ΔH of 90.0 and 135.3 mT for Ni/Y-Al and NiRh/Al, respectively. In view of the literature data [23], the most probable reason for the appearance of the signal Si2 is the presence of ferromagnetic metallic nickel. Compared with other samples, the signal Si1 of Ni/Y-Al is dominant. Therefore, a small number of nickel ions were reduced to metallic nickel for this sample. It may be concluded that nickel and yttrium interacted with each other and this led to a decrease of the reduced capacity of nickel oxide species. Addition of rhodium to the samples increased the reduction of Ni^{2+} to Ni^0, which was confirmed by the more pronounced signal Si2 in the

EPR spectrum of Ni-Rh/Al sample that is caused by the hydrogen spillover effect.
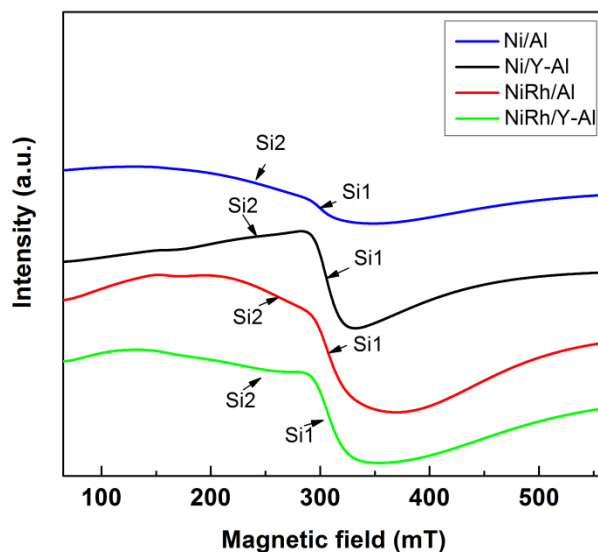
Fig. 3. EPR of reduced Ni-containing samples.

TPR profiles of calcined mono and Ni, Rh, and bimetallic NiRh samples are shown in figure 4. At a temperature above 450 °C a high hydrogen consumption with poorly resolved maxima at about 526, 600, 700, and 797 °C is observed for Ni/Al sample. Both higher temperature maxima should be related to hard reduction of nickel oxide species in strong interaction with alumina surface or to the presence of agglomerated NiO particles, whereas the lower temperature peaks at 526 and 600 °C are associated with the presence of small weakly bonded NiO species to the support. Addition of yttrium to Ni/Al gave rise to a shift of the latter two peaks to higher temperatures: from 700 to 725 °C and from 797 to 833 °C, respectively (Fig. 4).
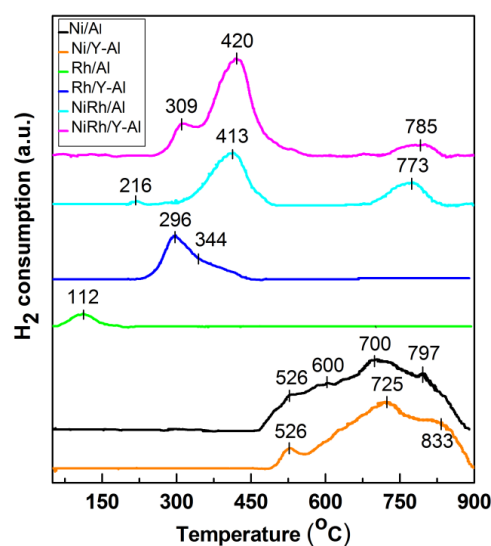
Fig. 4. TPR profiles of supported monometallic Rh and Ni and bimetallic RhNi samples.

The high temperature shift suggests a strong interaction between nickel oxide species and alumina support modified with yttrium. A TPR profile of Rh/Al sample demonstrated a small peak at around 112 °C assigned to reduction of rhodium oxide species. After introduction of yttrium to alumina, the TPR profile of Rh/Y-Al sample displayed a main signal at 296 °C with a shoulder at about 344 °C that corresponds to reduction of rhodium oxide species of different extent of interaction with yttrium-modified alumina support. No peaks were registered in the TPR profile of alumina modified with Y. As can be seen in figure 4, Rh improved Ni reducibility in the bimetallic RhNi sample by decreasing significantly the reduction temperature of nickel oxide species to 413 and 420 °C for NiRh/Al and NiRh/Y-Al, respectively, due to hydrogen spillover effect. It can be concluded that yttrium presence makes difficult the reduction of nickel and rhodium oxide species.

SUMMARY

Investigated monometallic Rh and Ni and bimetallic RhNi samples exhibited mesoporous structure. Supported yttrium oxide species were in amorphous state. Detected Ni^{2+} ions occurred in tetrahedral and octahedral configuration, similarly to surface $Ni_2Al_2O_4$ spinel structure and NiO, respectively. A strong interaction between yttrium oxide species and alumina was detected. A couple of Ni^{2+}/Ni^0 ions was defined in reduced Ni-containing samples based on EPR study. The reducibility of nickel oxide species increases in the presence of noble metal.

REFERENCES

1. J. R. Rostrup-Nielsen, J. H. B. Hansen, *J. Catal.*, **144**, 38 (1993).
2. H. Braga, J. B. O. Santos, J. M. C. Bueno, S. Damyanova, *Bulg. Chem. Commun.*, **49**, 45 (2017).
3. S. Damyanovaa, B. Pawelec, R. Palcheva, Y. Karakirova, M. C. Capel Sanchez, G. Tyuliev, E. Gaigneaux, J. L. G. Fierro, *Appl. Catal. B: Environ.*, **225**, 340 (2018).
4. N. Wang, K. Shen, L. Huang, X. Yu, W. Qian, W. Chu, *ACS Catal.*, **3**, 1638 (2013).
5. I. Luisetto, S. Tuti, C. Battocchio, S. Lo Mastro, A. Sodo, *Appl. Catal. A: Gen.*, **500**, 12 (2015).
6. M. L. Dieuzeide, M. Laborde, N. Amadeo, C. Bonura, F. Frusteri, *Int. J. Hydrogen Energy*, **41**, 157 (2016).
7. A. N. Fatsikostas, D. I. Kondarides, X. E. Verykios, *Catal. Today*, **75**, 145 (2002)
8. F. Can, A. Le Valant, N. Bion, F. Epron, D. Duprez, *J. Phys. Chem.*, C **112,** 14145 (2008).
9. S. Damyanova, B. Pawelec, K. Aristirova, J. L. G. Fierro, C. Sener, T. Dogu, *Appl. Catal. B: Environ.*, **92**, 250 (2009).
10. S. Damyanova, B. Pawelec, K. Arishtirova, J. L. G. Fierro, *Int. J. Hydrogen Energy*, **36**, 10635 (2011).
11. J. Zhang, H. Wang, A. K. Dalai, *J. Catal.*, **249**, 300 (2007).
12. Z. Hou, P. Chen, H. Fang, X. Zheng, T. Yashima, *Int. J. Hydrogen Energy*, **31**, 555 (2006).
13. G. Leofanti, M. Padovan, G. Tozzola, B. Venturelli, *Catal. Today*, **41**, 207 (1998).
14. A. Saric, S. Popovic, R. Trojko, S. Music, *J. Alloys Comp.*, **320**, 140 (2001).
15. Tisoaga, D. Visinescu, B. Jurca, A. Ianculescu, O. Carp, *J. Nanopart. Res.*, **13**, 6397 (2011).
16. K. T. Ng, D. M. Hercules, *J. Phys. Chem.*, **80**, 2094 (1976).
17. Y. Oh, H. Roh, K. Jun, Y. Baek, *Int. J. Hydrogen Energy*, **28**, 1387 (2003).
18. S. Eriksson, S. Rojas, M. Boutonnet, J. L. G. Fierro, *Appl. Catal. A: Gen.*, **326**, 8 (2007).
19. C. D. Wagner, L. E. Davis, M. V. Zeller, J. A. Taylor, R. H. Raymond, L. H. Gale, *Surf. Interface Anal.*, **3**, 21 (1981).
20. F. Can, A. Le Valant, N. Bion, F. Epron, D. Duprez, *J. Phys. Chem., C*, **112**, 14145 (2008).
21. A. J. A. Konings, W. L. J. Brentjens, D. C. Koningsrerger., V. H. J. De Beer, *J. Catal.*, **67**, 145 (1981).
22. D. S. Thakur, B. Delmon, *J. Catal.*, **91**, 308 (1985).
23. S. Damyanova, A. A. Spojakina, D. M. Shopov, *Appl. Catal.*, **48**, 177 (1989).

ФИЗИКОХИМИЧНИ СВОЙСТВА НА МОНОМЕТАЛНИ Ni И Rh И БИМЕТАЛНИ NiRh КАТАЛИТИЧНИ МАТЕРИАЛИ, НАНЕСЕНИ ВЪРХУ НЕМОДИФИЦИРАН И МОДИФИЦИРАН С ИТРИЙ АЛУМИНИЕВ ОКСИД

Р. Палчева, И. Щерева, Й. Каракирова, Г. Тюлиев, С. Дамянова*

Институт по катализ, Българска академия на науките, ул. „Акад. Г. Бончев", блок 11, 1113 София, България

(Резюме)

Изучен е ефектът на Y_2O_3, добавен в носител γ-Al_2O_3, върху структурата, повърхностните и редукционните свойства на нанесени монометални Rh и Ni и биметални RhNi каталитични материали. Използвани са различни техники за тяхното физикохимично охарактеризиране: адсорбционни-десорбционни изотерми на азот, дифузно отражателна и рентгенова фотоелектронна спектроскопия, електронен парамагнитен резонанс и температурно програмирана редукция. Установено е, че Ni^{2+} йони в накалени образци са в октаедрично и тетраедрично обкръжение, съответстващо на това в NiO и $NiAl_2O_4$ шпинел. Присъствието на двойка йони Ni^{2+}/Ni^0 е регистрирано с помощта на ЕПР в оксидни Ni-съдържащи образци. Наблюдавано е силно взаимодействие между Ni и Y_2O_3, проявяващо се в по-трудна редукция на никелови оксидни частици. Промотиращият ефект на Rh върху високата редуцируемост на NiO до Ni^0 се дължи на спиловер ефект на благородния метал.